Numerical Study of Quench Protection Schemes for an MgB_2 Superconducting Magnet

Mihailo Ristic*, John McGinley, Federico Lorenzoni

Imperial College London, Mechanical Engineering Department
South Kensington Campus, Exhibition Road, London SW7 2AZ, United Kingdom
+44 (0) 20 7 594 7048, m.ristic@imperial.ac.uk

***Abstract*—Thermal stability and protection in the event of quench are key issues in the design of superconducting magnets. Quench development and propagation strongly depend on the conductor characteristics and the magnet configuration. An adequate quench protection method must maintain both the peak temperature and the peak voltage during the event within acceptable limits. This paper presents quench modelling and evaluation of candidate protection schemes for a superconducting coil based on Magnesium Diboride (MgB_2) wire, designed for use in a new, cryogen-free, magnetic resonance imaging (MRI) scanner. The wire properties are different and the current density significantly higher from those previously reported. In contrast to previous studies it is concluded that the coil cannot be considered self-protecting and that protection using external resistance provides a practically acceptable solution.**

***Index Terms*— MgB_2 wire, superconducting coil, electromagnetic/thermal simulation, quench protection.**

I. Introduction

The interest in using high temperature superconductors (HTS) for the construction of magnets for applications such as Magnetic Resonance Imaging (MRI) and Magnetic Resonance Spectroscopy (MRS) has increased considerably in recent years. In particular Magnesium Diboride (MgB_2) appears to be one of the most promising materials for the construction of practical magnets in the near to medium term [1] and some such systems have become commercially available [2]. The critical temperature, T_c, of MgB_2 is 39 K, while the practical operating temperature in the presence of the required field and current may be between 10 K and 25 K, depending on the specific requirements and detailed design. This is considerably lower than, for example, YBCO (Yttrium Barium Copper Oxide) with T_c of 93 K, but it does offer important practical advantages in comparison with NbTi, the material used in the vast majority of superconducting magnets today and operating at 4.2 K or lower.

In applications such as MRI, provision of a cryogen-free magnet is highly desirable, as pressure vessel certification of the cryostat and the need to provide helium venting in case of quench contribute significantly to the cost of the installation. In the case of MgB_2, the operating temperatures are sufficiently high to allow direct cooling of the magnet coils by a conventional

* Corresponding author

cryocooler, with a sufficient quench margin to provide reliable operation in practice. This has been shown to be difficult to achieve using NbTi, which inevitably operates with very small margin, while each quench event can be costly due to the consequent machine down time – often of the order of weeks.

MgB_2 wire with suitable characteristics is already in commercial production. Made using the powder-in-tube process, it can be manufactured in sufficient lengths for magnet construction (several kilometres) and at a sufficiently low cost. These criteria have been hard to meet by other HTS materials.

The occurrence of quench, the transition of the material from superconducting to normal state due to a mechanical or thermal disturbance, can represent a serious issue during magnet operation. It is known that the normal zone propagation in HTS is slower than in low temperature superconductors (LTS) [3], with the result that the energy stored in the magnet may be dissipated in only a part of the volume occupied by the coil, causing significant local heating. The peak temperature, as well as the internal voltage rise, can reach high values that may irreversibly damage the integrity of the magnet [4]. For this reason it is important that a magnet quenches safely and an adequate protection of its thermal stability must then be arranged and built in. Several numerical models for the simulation of quench propagation in superconducting materials have been proposed [5],[6].

The work presented in this paper was conducted as part of the design of a 0.5 T open MRI magnet using MgB_2 superconductor. The project is being funded by the UK government Technology Strategy Board and aims to produce a compact, low-cost, open-magnet MRI system, suitable for installation within hospital Emergency Departments and for use in stroke diagnosis, trauma or for applications such as population screening in primary care centres. Importantly, the cryostat has been designed to be cryogen-free, with the coil being cooled directly by the cold head of the cryocooler. The design of the magnet has now been completed and it is being prepared for manufacture.

Since there has been relatively limited practical experience available with MgB_2 material, there were questions posed in relation to the quench performance and adequate quench protection methods for the specific coil design under consideration.

Most of the relevant work reported in the literature was based on using MgB_2 in the form of tapes[7],[8], while for this project it was decided to use a rectangular (1 mm x 2 mm) cross-section wire (supplied by Columbus Superconductors SpA, Italy). The wire has a matrix composed mainly of Monel (Table I) and presents very different physical properties from the tape, in particular a higher resistivity and a critical current that can reach values of more than 1000 A. This wire was chosen with the aim of achieving much higher average current density, reduced anisotropy effects, while the cross-section aspect ratio also lends itself to easier coil winding than some other geometries (e.g. square).

In subsequent sections we present the simulation study that was carried out and the design analysis in relation to three candidate quench protection methods. Details of wire characteristics and magnet properties are outlined in Section 2. The physics of the quench phenomenon is characterised by nonlinear, coupled, electromagnetic and thermal interactions that were modelled using equations outlined in Section 3. They were implemented in a Finite Element (FE) model using Comsol Multiphysics, taking into account the non-linearity of the material properties, while the time-varying circuit models were implemented using Matlab and coupled with the FE model. The remainder of the paper provides presentation and discussion of the results.

II. Wire Characteristics and Magnet Configuration

A. Overall magnet configuration

The configuration of the MRI magnet is unusual in that it employs a single driver coil, within a single cryostat, incorporated in the bottom pole. Both poles are specially designed to shape the field and achieve the required high uniformity within the imaging

volume. The magnet was designed to produce 0.5 T in the imaging volume of 20 cm diameter, 40 cm pole gap. The overall arrangement is shown in Fig.1, indicating the position of the cryostat containing the MgB_2 coil, while all other indicated parts are at room temperature.

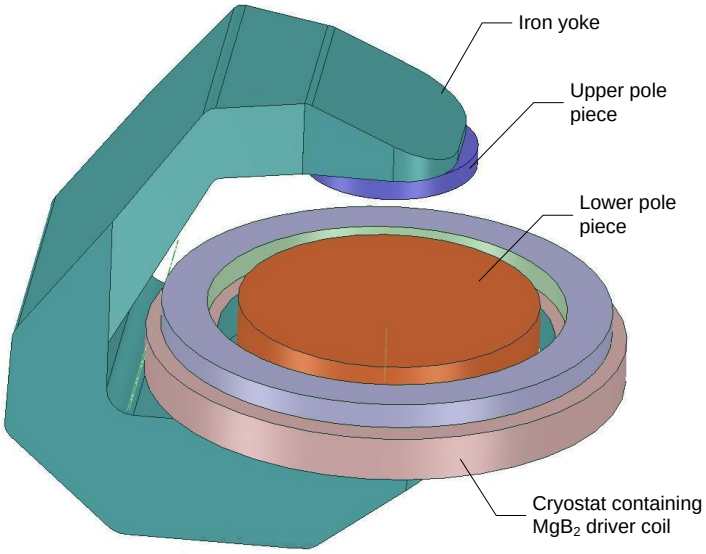

Fig. 1. Configuration of the prototype MRI magnet.

B. Wire configuration

The cross-section of the wire used in the magnet winding is shown in Fig.2. The conductor consists of 12 filaments of MgB_2, representing 10% of the overall cross-sectional area, embedded in a matrix of stabilizing magnetic materials. The wire also contains a central core made of copper. Table I lists the wire constituent materials and their relative proportions by mass.

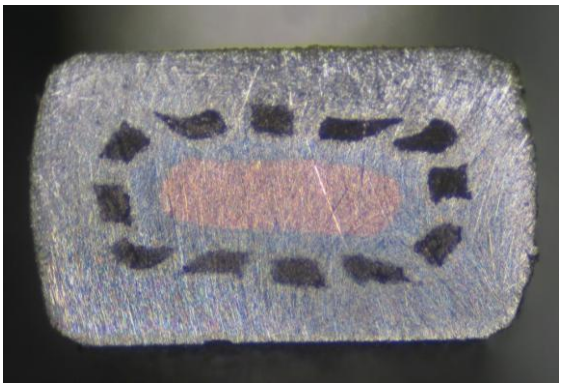

Fig. 2. Cross section of the 1mm × 2mm rectangular MgB_2 wire used.

TABLE I
WIRE COMPOSITION BY MASS

MgB_2	Copper	Monel	Nickel	Iron
13.5%	12.5%	43.5%	22.5%	8%

C. Wire physical properties

The conductor used for the coil manufacturing exhibits nonlinear physical properties, characterized by a strong dependency on temperature.

The critical current curves presented in Fig. 3 have been provided by the manufacturer, Columbus Superconductors. Parts of the graph have been extrapolated for the purposes of this work as they were not available from experimental measurements. This is the source data which is interpolated to obtain the step function $\delta(B,T, I)$ (see Section III) used in the model to determine which parts of the coil are in the normal state.

The thermal conductivity in particular is highly anisotropic. The reasons for this are the conductor layout and the fact that the wires in every turn are surrounded by a layer of insulating material. The longitudinal value of the thermal conductivity can be obtained through measurements while conductivities in the transverse directions must be computed using a model of the wire cross-section, insulating material (Dacron in this case) and the packing density of the winding in combination with the properties of the potting resin. The latter were obtained from the measurements made on a test coil, which was wound, potted and then cut to reveal the detailed structure of the windings. Thus the anisotropic thermal conductivity was evaluated on this basis using the method suggested in [9], while the heat capacity was averaged over the coil volume according to its percentage composition of various materials.

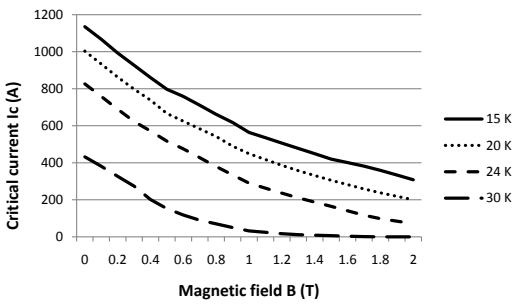

Fig. 3. Critical current I_c as a function of temperature and magnetic field magnitude B.

C. Coil configuration

The circular coil has a non-rectangular cross-section, as indicated in Fig.4, which was designed to limit the peak field to around 2 T. The coil has an inner diameter of 960 mm and cross-section before overwrap of 105 mm radially by 59 mm height; there is a staircase filler piece made of glass reinforced plastic on the upper inner radius of the coil. The coil is made up of 1680 turns, 80 layers, of insulated conductor assumed to be at the top tolerance limit (i.e. dimensions 2.1 mm × 1.01 mm) and covered with Dacron insulation which is nominally 0.13 mm thick. Moreover the coil is epoxy-impregnated. The insulated conductor dimensions are 2.36 mm × 1.27 mm and the turns are assumed to be packed closely. The present design also allows for quench heaters to be incorporated. Their function would be to speed up the quench propagation with the aim of spreading the heat dissipation throughout the coil and reducing the hot-spot temperature. Being made from thin copper film, they do not significantly affect the coil dimensions and other properties. In our studies we considered a situation involving ten secondary quench heaters positioned on the outer surface of the magnet and energized externally.

In the present design the coil will operate in non-persistent mode, since adequate methods for realising superconducting joints for MgB_2 wires are not yet available. This requires a current-source power supply to energize the magnet throughout its operation and has implications on the choice of suitable quench protection schemes.

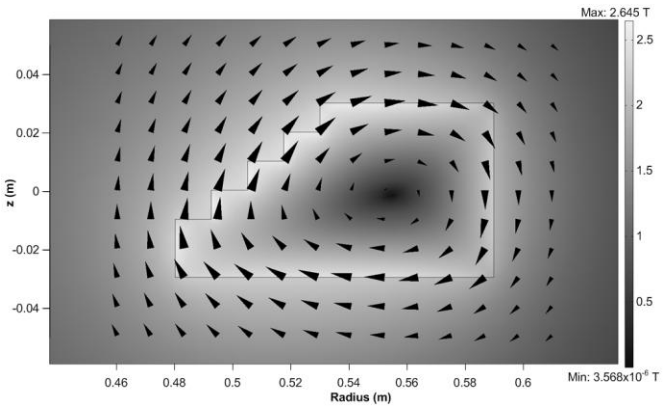

Fig. 4. Coil cross section with field ***B*** computed at full current.

III. Mathematical Model

A. Quench equations

The interdependence of different physical phenomena in the coil was modelled numerically using two modules. The electromagnetic module involved two-dimensional model of the coil cross-section, which was sufficient owing to the axisymmetric coil shape, and feeds the three-dimensional model of the thermal module.

The magnetic flux density can be expressed in terms of the magnetic vector potential ***A*** as:

$$\boldsymbol{B} = \nabla \times \boldsymbol{A} \qquad (1)$$

The magnetic field intensity ***H*** and the externally generated current density ***J*** are related by Ampere's law:

$$\nabla \times \boldsymbol{H} = \boldsymbol{J} \qquad (2)$$

B and ***H*** are related by the constitutive law:

$$\boldsymbol{B} = \mu \boldsymbol{H} \qquad (3)$$

where μ is the material magnetic permeability. From (1) – (3) a second order partial differential equation can be derived:

$$\nabla \times \left(\mu^{-1} \nabla \times \boldsymbol{A}\right) = \boldsymbol{J} \qquad (4)$$

Equation (4) may be solved numerically for a given coil geometry, using commercial FE packages. In this work COMSOL was used to set up a 2D axisymmetric model and to compute the magnetic field maps over the magnet cross section for different values of the current (Fig. 4).

Since it is impractical to model the detailed structure of the conductor for a large number of turns, a uniform current density was considered in the wire section. Using magnetization curves of actual MgB_2 samples measured in a laboratory by the wire manufacturer, a nonlinear permeability function $\mu(B)$, where B is the magnitude of $\boldsymbol{B}$, was derived which was incorporated into this 2D model. Since the coil was to be represented as a homogenized magnetic material, the magnetization was first diluted by the net coil packing factor of 64% to reflect the insulation between turns of the coil. At any given current density $\boldsymbol{J}$, a flux density $\boldsymbol{B}$ could then be computed in the wire which reflected its magnetic composition, as shown in Fig.4. This magnetic field information could then be fed into the computation of heat generation in the next stage.

A 3D thermal model represents the effective bulk coil and the thermal propagation of quench and this is ruled by the heat flow equation:

$$dc_p(T)\frac{\partial T}{\partial t} - \nabla \cdot (k(T)\nabla T) = Q \qquad (5)$$

in which d represents the material density, c_p the heat capacity at constant pressure and T the temperature. k is the tensor representing anisotropic thermal conductivity, which in the coil circumferential direction corresponds the properties of the wire, while in the coil radial direction it was obtained by averaging volumetric fractions of the constituents, including the wire and the insulation. Q is the thermal power generation, computed as

$$Q = J^2 \rho(T)\delta(B,T,I) \qquad (6)$$

where $\rho(T)$ indicates the normal state electrical resistivity and I is the total current in the conductor. $\delta(B,T,I)$ is a step function which discriminates between the points of the coil in the region where quench has been initiated and the fully superconducting region, based on the critical surface characteristics. This function $\delta(B,T,I)$ is computed at all stages of the quench evolution in all 3D locations of the coil using manufacturer's critical current data (Fig 3), interpolated in the dimensions of B and T to find $I_c(B,T)$. Thus for an operating current I, at a particular point in the coil:

$$\delta(B,T,I) = \begin{cases} 0 & \text{if } I < I_c(B,T) \\ 1 & \text{if } I \geq I_c(B,T) \end{cases} \qquad (7)$$

The regions of the coil where $\delta(B,T,I) = 1$ may be either in a fully normal state, or in a transition state whereby the current I is shared between the superconductor and the matrix.

Literature suggests two main current sharing models that may be appropriate.

1. Assume that all current in the wire in excess of $I_c(B,T)$ is carried by the matrix and there is no resistive heat generated in the superconductor material itself.

2. Assume that the wire current in excess of $I_c(B,T)$ is also carried by the superconductor material. This current is then shared between the parallel resistances offered by the superconductor and the matrix, generating heat in both.

The first current sharing model was found to be appropriate when there is a sharp voltage-current transition of the superconducting filament and when the electrical resistivity of the matrix is much lower than the normal state resistivity of the filaments. The sharpness of the voltage-current transition is characterised by the n-value in the empirical expression $V \propto I^n$.

It has been widely suggested [10] that the first model is appropriate for LTS including NbTi and NbSn because they usually have high n-value and wires use copper matrix, making the matrix resistivity relatively low. It has also been suggested that the second model is more suitable to HTS such as YBCO and BSCCO. However, for MgB_2 the appropriate choice of the model is not obvious [10] and it depends on the particular properties of the wire in question.

In the case presented here, there was limited measurement data available for the wire and we had to exercise judgement. The available data from the manufacturers (Fig 3) indicates that very high critical current of 1200 A is achievable at 15 K and even higher value may be extrapolated at 10 K, with the corresponding current density of 6×10^4 A/cm^2 or higher. In a recent paper [11], Kim *et al.* studied the correlation between the critical current density J_c and the n-value in MgB_2/Nb/Monel superconductor wires. They concluded that the power law $n \propto J_c^m$ applies, where m was approximately 0.371. Using the results presented in [11] it was concluded that $n > 30$ may be assumed for the wire considered in this case. Furthermore, the inclusion of the copper core in the wire construction results in a significant reduction in the matrix resistivity when compared to using Monel alone. Therefore on the basis of both considerations it was concluded that the first current sharing model would be appropriate in this case.

Following this, the current density J used in (6) is calculated as

$$J = \frac{I - I_c(B,T)}{A_{cond}} \qquad (8)$$

where A_{cond} is the cross sectional area of the matrix.

The discretised coil model consisted of a mesh of around 2500 elements for the 2D electromagnetic model and 48000 elements for the 3D thermal model.

B. Quench protection electrical circuit

As mentioned previously, the magnet is designed to operate in non-persistent mode and the required current-source power supply must be disconnected as soon as the quench event is detected. The candidate quench protection schemes that were analyzed were self-protecting coil, protection using external resistance and protection using externally energized quench heaters.

The electrical circuit shown in Fig. 5 was used in relation to all three cases, where the current source I_s is the magnet power supply, R is the resistance of the coil due to the normal zone and R_{ext} of an appropriate value is the external resistance. In normal operation, switch S is closed and current flows around the magnet coil L (inductance 12 H, assumed constant) – in this mode Diode D prevents current flow through $R_{ext.}$ When a quench voltage is detected across the magnet, S is opened and the magnet current decays via R_{ext}. In the cases where external resistance is not employed, $R_{ext} = 0$.

In practice, the switch S will be implemented using a fast, solid-state device such as the insulated gate bipolar transistor (IGBT) and for the purposes of this study its operation may be considered almost instantaneous. It will be controlled by the magnet control system, which detects the quench event as a rise in the coil terminal voltage from an initially very low value to

one above some predefined threshold (usually 1 – 3 V). The threshold voltage is selected to be as low as possible in order to minimise the reaction time and it should be high enough to prevent spurious shutdowns due to noise. The threshold was set to 3 V in all simulations presented here.

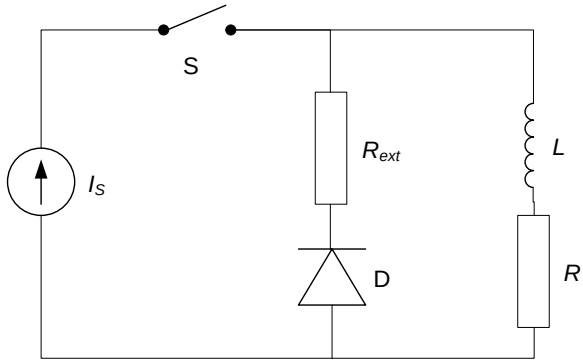

Fig. 5. Electrical circuit model.

Following the detection of the rise in coil voltage and the opening of the switch, the time dependent value of the current in the magnet coil is evaluated according to the Kirchoff's second law :

$$L\frac{dI}{dt}+\left(R+R_{ext}\right)I(t)=0 \qquad (9)$$

where

$$R=\frac{\int_{\Omega}J^{2}\rho(T)\delta(B,T,I)d\Omega}{I^{2}} \qquad (10)$$

is the resistance of the normal zone calculated on the coil volume Ω, R_{ext} is an external shunt resistor and L is the coil inductance. The current density J at any given point is computed using (8)

Equation (9) accounts for the coil current decay due to the increase in the coil resistance during quench, which causes a reduction in the field B and affects the further propagation of the normal zone. It is solved iteratively, as part of the overall simulation loop (Fig. 6), involving time increments Δt. At every solution time step i, interval Δt, the value of the current is recalculated as:

$$I_i = I_{i-1} - I_{i-1}\left(R_{i-1}+R_{ext}\right)\frac{\Delta t}{L} \qquad (11)$$

The coil terminal voltage at each time step is calculated as the product $I_i R_i$.

C. Overall simulation loop

The overall structure of the iterative simulation loop is shown in Fig. 6. Initially, the current is set to the design value of 175 A and the quench is initiated at time t = 0 as a pulse of localised heat flux of short duration. The iterative simulation loop consists of three main steps. The first step involves the solution of the 2D electromagnetic model using the instantaneous coil current I as

the input and it calculates the corresponding magnetic field B as the output. This provides the link to the second step, the 3D thermal model, in which the function $\delta(B,T,I)$ is evaluated at all points in the model to identify the normal and the superconducting parts of the coil. Resistive heating Q and the rise in temperature T are also calculated. The coil resistance R is then calculated as the output of this step, using (10). The third simulation step solves the circuit model using (11) to calculate the new value of the current, used in the next iteration of the loop. The simulation is terminated when the current drops to below 1 A.

The electromagnetic and thermal models of the coil were implemented using Comsol Multiphysics, whereas the circuit model and other algorithm logic were implemented in Matlab.

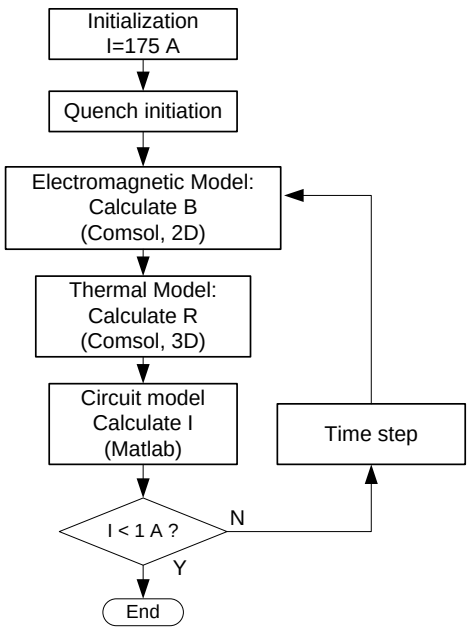

Fig. 6. Overall simulation structure.

IV. Simulation and Results

The quench initiation event was a thermal disturbance modelled as a short burst of heat flux applied for 0.2 s in a small portion of a conductor positioned on the inner surface of the coil (the leftmost side of the coil cross section in Fig. 4).

The quench detection criterion was set to 3V and it was reached in the region 200-330 ms after quench initiation in all cases. At that instant the switch S in Fig.5 is opened. The coil operating current at which quench occurs was 175 A. Two different operating temperatures of 10 K and 15 K, uniform throughout the coil volume, were considered to define the likely range for this magnet.

The simulations were conducted in order to investigate different quench protection schemes, where the main quantities of interest were the peak temperature and the peak voltage. Three candidate schemes were analysed:

- self-protecting coil, short circuit ($R_{ext} = 0$)
- protection using external dump resistance $R_{ext} = 5$ Ohm
- protection using externally powered quench heaters, short circuit ($R_{ext} = 0$)

Fig. 7 shows typical coil temperature distribution at the end of the simulation. Figures 8(a – h) summarise the main results, showing the evolution current, resistance, peak temperature and voltage for the three quench protection cases and for the two operating temperatures.

The target for the peak allowable temperature was set based on experience. A comparable NbTi coil was simulated and shown that under quench it would reach peak temperature of 50 K and a fairly uniform circumferential temperature distribution (cf. Fig 7), owing to a rapid longitudinal quench propagation. With this in mind and in view of the expected propagation rates for MgB_2, the maximum allowable peak temperature was set at 200 K, which was considered compatible with maintaining coil integrity.

The other consideration was the voltage rise across the coil, for which 600 V was considered to be acceptable from the point of view of coil insulation. In addition, overvoltage may be an issue for the magnet power supply. The commercial units under consideration include suitable circuits capable of protecting the power supply from coil voltages of 400 – 600 V, depending on the model. It was therefore desirable to limit voltage rise to below these values, making the power supply protection independent of the operation of switch S.

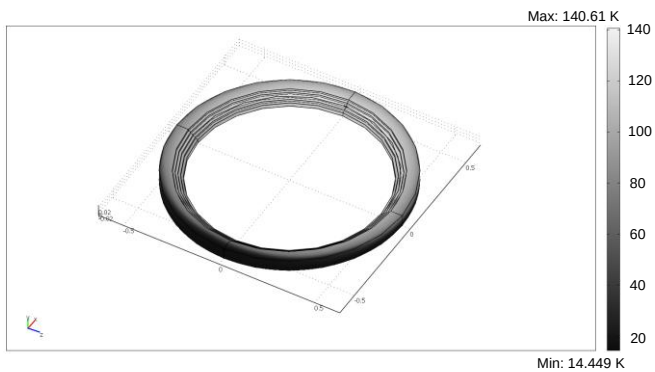

Fig. 7. Coil temperature distribution following quench.

A. Self-protecting coil

Simulations have been performed in the first instance involving a short circuit (R_{ext} = 0), with the magnet otherwise unprotected. The results are shown by the solid lines in the graphs in Fig. 8 (a-d) for the operating temperature of 10 K and Fig. 8 (e-h) for 15 K. It can be seen that the current decay times are short, only of the order of a few seconds. However the hot-spot temperature can be seen to rise well above 200 K for both initial temperatures. Also, the voltage in this case can be seen to rise to the region of 1100–1200 V and therefore far in excess of the prescribed limits.

B. External resistance

In the second set of simulations, a 5 Ohm external shunt resistor was switched in following the quench detection, in order to facilitate the extraction of the magnet energy. The results are shown by the dotted lines in the graphs in Fig. 8 (a-h). The presence of the shunt resistor reduces both the magnet hotspot temperature and the peak voltage considerably. Overall, it can be concluded that this scheme is highly effective, with the peak temperature limited to well below 180 K, while the peak voltage is reduced to acceptable levels of 80–160 V.

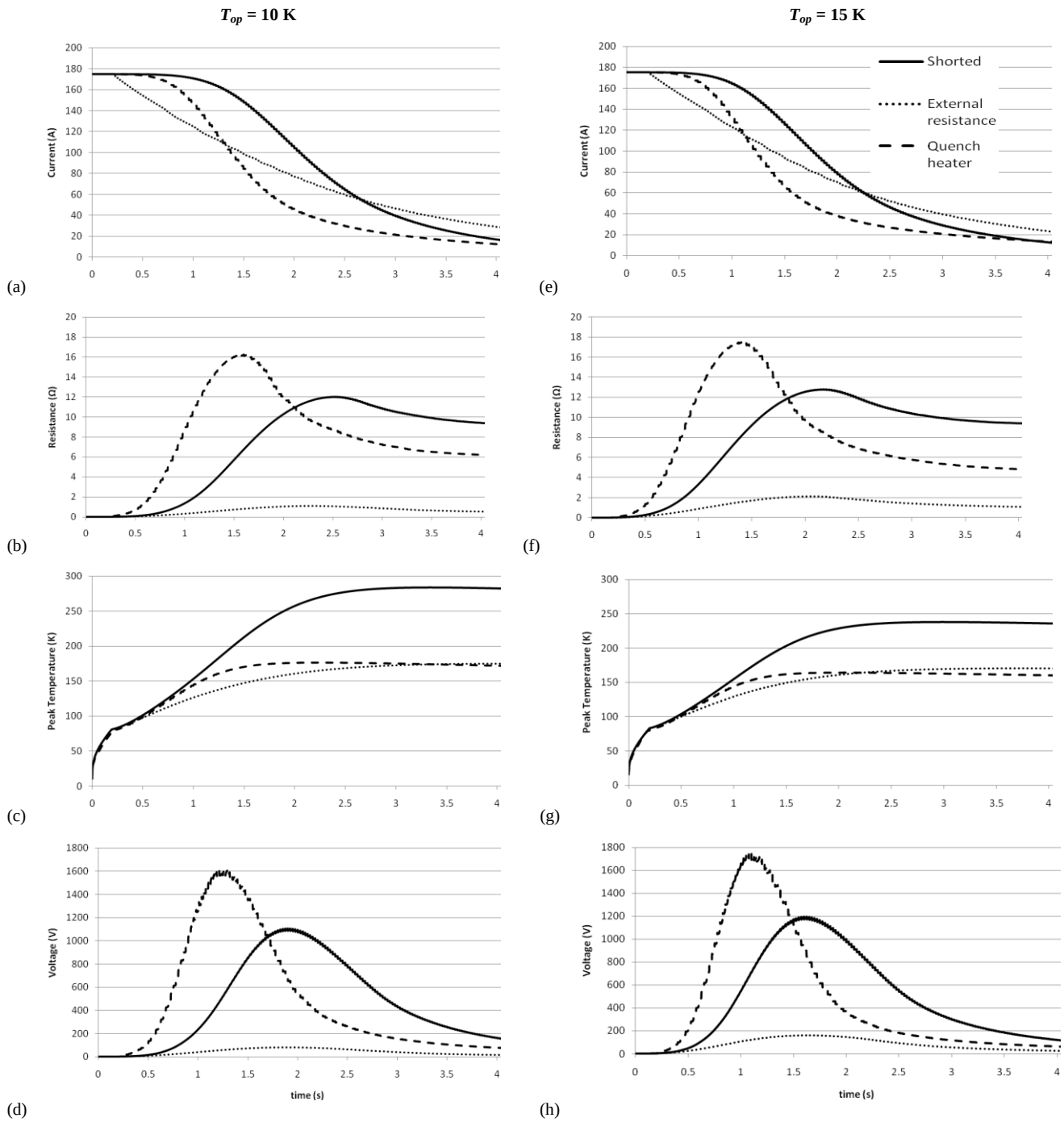

Fig. 8. Quench simulation results at the operating temperatures of (a-d) 10 K and (e-h) 15 K. Solid lines describe the self-protecting coil, dotted lines describe quench protection using external resistance R_{ext} =5 Ohm and dashed lines describe quench protection using quench heaters.

C. Quench heaters

In the last case to be investigated, the protection scheme consisted of ten secondary quench heaters each generating 150 W positioned on the outer surface of the magnet and energized for 0.8 s after the quench has been detected. The heaters have the function to speed up the quench propagation with the aim of spreading the heat dissipation throughout the coil and reducing the hot-spot temperature. The results are shown by the dashed lines in the graphs in Fig. 8 (a-h).

Simulation results show that this method reduces the current decay time by 10-20 %, compared to the self-protecting coil, as an effect of the increased coil resistance. The peak temperature is also reduced significantly, to below 180 K and therefore within the prescribed limits. However, the peak voltage can be seen to be significantly higher than in either of the previous cases, in the range 1600–1800 V, which is not compatible with the prescribed range of operation.

V. Conclusion

The performance of superconducting coil under quench conditions and the effectiveness of candidate protection methods are difficult to predict without resorting to detailed numerical simulation studies. In view of the limited prior experience with MgB_2 superconductors, the analysis presented in this paper was conducted as part of the design process for a novel MRI magnet system.

Since it is known that quench propagation in MgB_2 wires is an order of magnitude slower than in low temperature materials, the primary concern at the outset was to limit the peak temperature in the coil. In this respect it was found that protection methods using external resistance and quench heaters are about equally effective, while the self-protecting coil is likely to reach peak temperatures above the acceptable limit. These conclusions differ from those achieved in previous analyses of MgB_2 tapes that suggested that the magnet could be considered self-protective [9]. The main reason is probably to be found in the very different values of the current densities between the two conductors and different thermal conductivities from those considered here.

For the wire and the conditions considered here, it is concluded that quench protection must remove a significant amount of stored energy from the coil in order to avoid overheating. This has increasingly strong implications with increasing stored energy in the coil. Previous studies which considered much lower currents were found to be self-protecting, but with a view of significantly increasing the current capacity in the future, the measures for safely extracting the energy during quench must be carefully considered.

It was also found that the voltage rise, rather than the temperature rise during quench can become the limiting factor for a given protection method, due to the resistance of the wire material.

For the simply wound coil considered here, it was encouraging to find that a conventional protection method involving external resistance will meet the performance criteria. However, this method is mainly applicable to non-persistent, externally energized coils, while it may not be suitable for persistent or quasi-persistent designs. In such cases, an approach that warrants further consideration would involve incorporating a significant amount of additional copper in the coil windings, mainly with the aim of limiting the voltage rise as well as improving the quench propagation speed.

Acknowledgment

This work has been supported by the Technology Strategy Board Grant No M1575C. The authors would like to thank Dr Giovanni Grasso at Columbus Superconductors SpA for providing the wire data and support for this work. We are very grateful to Professor David Caplin at Imperial College for his guidance and advice. Special thanks also to Dr Antti Stenvall at Tampere University of Technology for his helpful advice.

REFERENCES

[1] M. Modica *et al.*, "Design, Construction and Tests of MgB_2 Coils for the Development of a Cryogen Free Magnet," *IEEE Trans. Appl. Supercond.*, vol. 17, no. 2, pp. 2196–2199, Jun. 2007.

[2] Paramed Medical Systems, www.paramed.it

[3] H. van Weeren. "Magnesium Diboride Superconductors for Magnet Applications" PrintPartners Ipskamp, Enschede. ISBN 978-90-365-2519-0 2007

[4] M. N. Wilson, *Superconducting Magnets*. Oxford: Clarendon Press, 1983.

[5] P. J. Masson *et al.*, "Development of Quench Propagation Models for Coated Conductors," *IEEE Trans. Appl. Supercond.*, vol. 18, no.2, pp. 1321–1324, Jun. 2008.

[6] S. Caspi *et al.*, "Calculating quench propagation with ANSYS," *IEEE Trans. Appl. Supercond.*, vol. 13, no. 2, pp. 1714–1717, Jun. 2003.

[7] M. Runde *et al.*, "MgB_2 coils for a DC superconducting induction heater," 8th European Conference on Applied Superconductivity (EUCAS 2007) Journal of Physics: Conference Series 97 (2008) 012159.

[8] A. Stenvall *et al.*, "Stability of MgB_2 Superconductor," *IEEE Trans. Appl. Supercond.*, vol. 16, no. 2, pp. 1399–1402, Jun. 2006.

[9] A. Stenvall, A. Korpela, R. Mikkonen, G. Grasso, Quench analysis of MgB_2 coils with a ferromagnetic matrix , Supercond. Sci. Technol. 19 (2006) 581–588.

[10] H. van Weeren, et al., "Adiabatic normal zone development in MgB2 superconductors," IEEE Transactions on Applied Superconductivity, vol. 15, pp. 1667-1670, 2005.

[11] J. Kim, et al., "Correlation between critical current density and n-value in MgB2/Nb/Monel superconductor wires," Physica C: Superconductivity, 2010.

List of Figures

Fig. 1. Configuration of the prototype MRI magnet.

Fig. 2. Cross section of the 1mm × 2mm rectangular MgB_2 wire used.

Fig. 3. Critical current I_c as a function of temperature and magnetic field.

Fig. 4. Coil cross section with field ***B*** computed at full current.

Fig. 5. Electrical circuit model.

Fig. 6. Overall simulation structure.

Fig. 7. Coil temperature distribution following quench

Fig. 8. Quench simulation results at the operating temperatures of (a-d) 10 K and (e-h) 15 K.

List of Tables

Table I: Wire composition by mass

Author Biographies

Mihailo Ristic

Mihailo Ristic graduated from University College London in 1981 with First Class Honours in Mechanical Engineering. He recieved M.Sc. in Control Systems in 1982 and Ph.D. in Robot Dynamics and Control in 1986, both from Imperial College London.

Since 1986 he has been a member of staff in the Mechanical Engineering Department at Imperial College where he is currently Senior lecturer. His research interests include a wide range of topics in Control systems, Computer Aided Design, electrical machines, as well as Magnetic Resonance Imaging and its applications. He is a co-founder of Turbo Power Systems who specialize in high-speed electric motors, generators and power electronics.

He is a Chartered Engineer, Fellow of the Institution of Mechanical Engineers and a member of IEEE since 1994.

John Vincent Mario McGinley

John Vincent Mario McGinley was born in Dublin in 1954. He received his B.A. degree in physics from University of York in 1976 and was awarded the D.Phil. degree from University of Oxford in 1980 with a thesis on tuneable dye laser spectroscopy at the Clarendon Laboratory.

He has worked on the design and development of many aspects of magnetic resonance imaging (MRI) technology such as magnets, shimming systems and gradient coils with Picker International, Marconi and Philips. He co-founded InnerVision MRI in 1994 which specialises in niche MRI systems and has also worked since then as a consultant in advanced magnetic design especially the optimisation software development for magnets fellowship at the Department of Mechanical Engineering, Imperial College, London.

Dr McGinley is a chartered physicist and a member of the Institute of Physics.

Federico Lorenzoni

Federico Lorenzoni received the M.S. degree in nuclear engineering from the University of Bologna, Italy, in 2003. Part of his Master research was done at the University of Tokyo in Japan on the subject of superconducting magnetic bearings for high temperature superconductors (HTS).

From 2006 to 2008 he was a Research Engineer at Aavid Thermalloy, LLC where he investigated novel cooling systems for electronics and thermal solutions for industrial applications. In 2008 he joined Imperial College London, United Kingdom, as Research Assistant for the project “Compact MRI system for accident and emergency”. His research interests include superconducting technology and heat transfer problems.